

Diffusivity of Ozone in Water

Paul N. Johnson[†] and Richard A. Davis*

Department of Chemical Engineering, University of Minnesota–Duluth, Duluth, Minnesota 55812

The diffusivity of ozone in water was determined experimentally by measuring the rate of ozone absorption into an aqueous laminar liquid jet. Penetration theory was used to interpret the results. Experiments were conducted over the temperature range of 10 °C to 45 °C. The results for diffusivity were correlated by an Arrhenius function for temperature dependence with a maximum deviation of $\pm 3.3\%$: $D/\text{m}^2\cdot\text{s}^{-1} = 1.10 \times 10^{-6} \exp[-1896/(TK)]$.

Introduction

Ozone (O_3) has been widely recognized as a powerful oxidizing agent, with applications in water treatment, disinfection, bleaching, and odor control, among others (Brink et al., 1991; Hill and Rice, 1982). Aqueous reactions with unsaturated hydrocarbons are often mass transfer limited due to the relatively low solubility of O_3 in water and fast reaction kinetics (Kuo and Yocum, 1982). Estimations of mass transfer coefficients for proper design of O_3 contactors require values for the diffusion coefficient of O_3 . The diffusivity of O_3 in water is also required to determine reaction rate constants from gas absorption experiments (Davis et al., 1995). In this work, new results for O_3 diffusivity in water are reported, which extend the range of temperature beyond previously reported values (Matrosov et al., 1976). The diffusivity was determined by applying penetration theory to experiments measuring the rate of O_3 absorption from the gas phase into a laminar liquid jet stream of water. Experiments were repeated over the temperature range of 10 °C to 45 °C. The results were correlated to an Arrhenius function for temperature dependence.

Gas Absorption Theory

According to Higbie's penetration theory, the average rate of O_3 gas absorption into liquid water is a function of the diffusivity of the dissolving gas in the liquid, the gas–liquid contact time, and the solubility of the gas in the liquid (Danckwerts, 1970):

$$r = 2S(C^* - C^{\circ})\sqrt{D/\pi\theta} \quad (1)$$

where C^* is the concentration of O_3 in water at the gas–liquid interface, C° is the bulk water concentration of O_3 , D is the diffusivity of O_3 in water, θ is the time of liquid exposure to the gas, and S is the interfacial area of absorption. In this work, liquid water is exposed to the ozone-laden gas in the form of a cylindrical, rodlike, laminar jet, where the interfacial area is

$$S = \pi dh \quad (2)$$

and where d is the jet diameter and h is the jet height. The jet exposure time is calculated from the volumetric flow

rate and jet dimensions:

$$\theta = \pi d^2 h / 4L \quad (3)$$

where L is the volumetric liquid flow rate. For short contact times, using pure solvent, the bulk concentration of dissolving gas is essentially zero. Substitution for S and θ from eqs 2 and 3 into eq 1 results in an expression for the average gas absorption rate, independent of jet diameter:

$$r = 4C^*\sqrt{DLh} \quad (4)$$

Local equilibrium between the gas and liquid is assumed at the interface. Ozone is sparingly soluble in water such that Henry's law is used to describe the physical equilibrium condition at the gas–liquid interface:

$$C^* = PC_w/H \quad (5)$$

where P is the partial pressure of O_3 in the gas, H is Henry's constant for O_3 solubility in water, and C_w is the total molar concentration of liquid, approximately that of water in this case. A correlation of Henry's constant was found from the results of Roth and Sullivan (1981):

$$H = 3.84 \times 10^7 [\text{OH}^-]^{0.035} \exp[-2428/T] \quad (6)$$

where the dimensions of H , T , and $[\text{OH}^-]$ are $\text{atm}\cdot(\text{mole fraction})^{-1}$, K, and $\text{mol}\cdot\text{L}^{-1}$, respectively. Equation 6 applies for the conditions of $4\text{ °C} < t < 60\text{ °C}$ and $1 < \text{pH} < 10$. Gas phase mass transfer resistance was ignored due to the relatively low solubility of O_3 in water. From boundary layer theory, the overall liquid phase mass transfer coefficient is

$$K_L = 1/(1/k_L + P_T/Hk_G) \cong k_L \quad (7)$$

where k_L and k_G are the average local liquid and gas phase mass transfer coefficients and P_T is the total pressure. Values for k_L and k_G were approximated from penetration theory and a correlation for flow past a flat surface (Incropera and DeWitt, 1996), respectively:

$$k_L = 2\sqrt{D/\theta} \quad (8)$$

$$k_G = 0.669(D_G/h)(4Lh\rho_G/\pi d^2\mu_G)^{1/2}(\mu_G/D_G\rho_G)^{1/3} \quad (9)$$

where the subscript G indicates gas phase properties, μ is the dynamic viscosity, and ρ is the density assuming ideal gas behavior. For typical values of these parameters, $k_L \approx 1 \times 10^{-3}$, $k_G \approx 1 \times 10^{-2} \text{ m}\cdot\text{s}^{-1}$, $P_T \approx 1 \text{ atm}$, and $H \approx$

* To whom correspondence should be addressed.

[†] Present address: Hutchinson Technology, Inc., Hutchinson, MN, 55350.

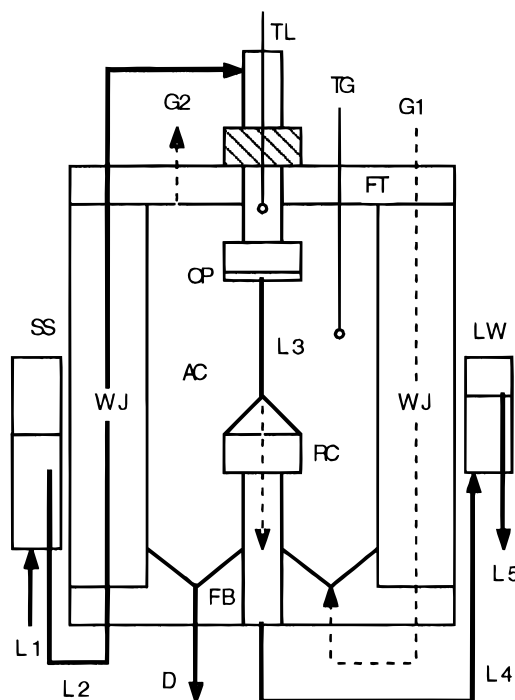


Figure 1. Laminar liquid jet absorber diagram: AC = gas absorption chamber, D = liquid drain, FB = bottom flange, FT = top flange, G1 = gas feed to water jacket and absorption chamber, G2 = gas to vent or spectrophotometer flow through cell, L1 = liquid feed to surge suppressor, L2 = liquid to water jacket and jet orifice, L3 = exposed laminar liquid jet, L4 = liquid to constant leveling ware or to spectrophotometer flow through cell, L5 = liquid out, LW = liquid constant leveling ware, OP = orifice plate, RC = liquid jet receiving tube, SS = liquid flow surge suppressor tank, TG = gas thermocouple, TL = liquid thermocouple, WJ = water jacket.

5000 atm·(mole fraction)⁻¹, indicating from eq 7 that essentially all mass transfer resistance resides in the liquid phase.

Experimental and Analytical Procedures

A laminar liquid jet absorber, similar to the one described by Al-Ghawas et al. (1989), was used to measure the rate of absorption of O₃ into water. Matrosov et al. (1976) also used a liquid jet absorber to study O₃ diffusion in water. The liquid and gas flow paths through the apparatus are illustrated in Figure 1. The materials of construction were Teflon, glass, Viton rubber, and 316 stainless steel, to prohibit reactions with O₃. The device was constructed by clamping concentric 0.10 m and 0.15 m diameter glass pipes between 0.05 m thick Teflon flanges. Viton rubber gaskets were used to seal the glass to the Teflon. The space inside the center pipe was used as the gas-liquid absorption chamber. The annulus between the pipes was used to control the temperature with circulating water from a temperature-controlled bath. Uniform liquid flow was maintained with a surge suppressor tank. Volumetric liquid flow rates were approximately 4 × 10⁻⁷ m³·s⁻¹. A laminar liquid jet was created by pumping the water through a 5.0 × 10⁻⁴ m thin square-edged orifice, constructed of stainless steel. The diameter of the orifice was 8.0 × 10⁻⁵ m. This orifice design was recommended by Raimondi and Toor (1959). The orifice plate was mounted at the end of a 0.01 m glass liquid feed tube with a Swagelok Teflon feruled nut. The liquid jet was collected through the center of a stainless steel cone at the end of a 0.01 m diameter glass riser tube. The inside diameter of the liquid receptacle was just larger than the

diameter of the orifice in order to restrict gas absorption only to the exposed liquid jet. The liquid level was maintained at the tip of the cone to prevent entrainment of gas, accomplished with a constant leveling ware positioned outside the device. The length of the jet was changed by adjusting the vertical position of the glass feed tube. Jet heights ranging from 0.010 m to 0.021 m were measured with a Titan cathetometer attached to a Starrett height gauge, precise to within ±5.0 × 10⁻⁶ m.

Only distilled, deionized water was used in the liquid feed. The water was first degassed by warming under vacuum. The acidity of the feed stock and absorber effluent was measured with a Mettler combination electrode pH probe. The pH varied from 5.8 to 6.2 between runs. Ozone was created by feeding 99% pure, dry O₂, supplied by GENEX, to a corona discharge type ozone generator, manufactured by Ozone Research and Equipment Corp. The O₃/O₂ gas stream from the generator was continuously introduced to the absorption chamber during any given run. The pressure was maintained near atmospheric. The gas and liquid streams were passed through coiled Teflon tubes inside the annulus before being introduced to the absorption chamber for additional temperature control. The gas and liquid temperatures were the same within ±0.3 deg. Experiments were conducted at 5 deg temperature increments over the range of 10 °C to 45 °C. Temperatures were measured with thermocouples placed in the gas chamber and liquid feed tube, precise to ±0.1 deg.

The rate of O₃ absorption was calculated from the volumetric flow rate of the effluent water and the concentration of O₃ in the effluent stream:

$$r = LC \quad (10)$$

The volumetric flow rate was found from the mass flow rate and liquid density, assumed to be that of pure water (Dean, 1992). The composition of the liquid was determined with a Hewlett-Packard 8453 diode array UV-visible spectrophotometer by measuring its absorbance at the 260 nm wavelength in the ultraviolet spectral range (Kuo et al., 1977). The aqueous O₃ concentration was calculated from Beer's law:

$$C = A_L / \epsilon b_L \quad (11)$$

where A_L is the liquid absorbance, ϵ is the absorptivity of O₃, and b_L is the spectrophotometer light path length through the liquid sample. A 0.1 m quartz flow cell was used to measure the absorbance of O₃ in the liquid water. The partial pressure of O₃ in the gas phase was also found by spectrophotometry, assuming ideal gas behavior:

$$P = A_G RT_c / \epsilon b_G \quad (12)$$

where A_G is the absorbance of the gas sample, R is the ideal gas constant, T_c is the absolute temperature of the gas in the spectrophotometer cell, and b_G is the spectrophotometer light path length through the gas sample. A 0.01 m quartz flow cell was used to measure the absorbance of O₃ in the gas. Assuming that the absorptivity of O₃ is the same in the gas and liquid phases eliminates this parameter from the calculations for diffusivity. Substitution from eqs 10-12 into eq 4, yields the following expression for diffusivity.

$$D = (L/h)[0.1A_L H^4 A_G C_w RT_c]^2 \quad (13)$$

A minimum of three experiments was performed at each temperature. This direct spectrophotometric method of analysis was confirmed by the indirect indigo dye method of Bader and Hiogné (1982). The liquid residence time

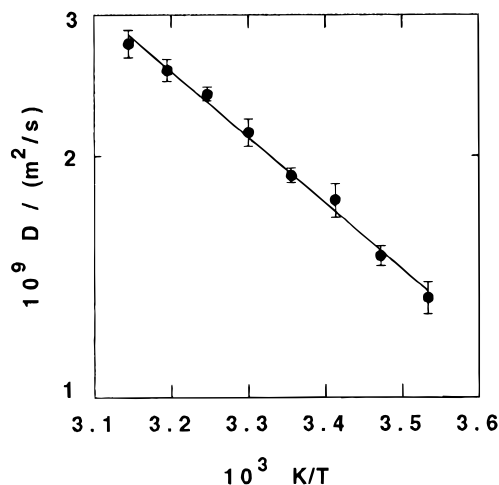


Figure 2. Arrhenius plot of O_3 diffusivity in water: (●) experiment; (—) eq 15 ($R^2 = 0.993$).

Table 1. Experimental Results for O_3 Diffusivity in Water, Experimental Standard Deviation, and Stokes–Einstein Constant

T/K	$10^9 D/m^2 \cdot s^{-1}$	$10^{11} \sigma/m^2 \cdot s^{-1}$	$10^{15} c/Pa \cdot m^2 \cdot K^{-1}$
283.5	1.33	6.1	6.16
288.1	1.50	4.4	6.00
293.1	1.76	8.4	6.13
298.2	1.89	4.1	5.78
303.3	2.14	8.5	5.77
308.0	2.39	4.7	5.73
312.9	2.56	8.2	5.48
318.2	2.76	11	5.30

between the absorption chamber and the spectrophotometer cell was less than 1 min. At 25 °C and a pH = 7, the half-life of O_3 is 20 min to 30 min in relatively pure water (Bablon et al., 1991). Therefore, the decomposition of O_3 was ignored in the analysis.

Results and Discussion

The mean experimental results for aqueous O_3 diffusion coefficients are listed in Table 1. The maximum error in the diffusivity was estimated at $\pm 5\%$. At 20 °C, Bablon et al. (1991) report a value for D of $1.74 \times 10^{-9} m^2 \cdot s^{-1}$ that compares favorably with the result of $1.76 \times 10^{-9} m^2 \cdot s^{-1}$ reported here. The standard deviation from the mean (σ) is also reported in the table along with the Stokes–Einstein constant:

$$c = D\mu/T \quad (14)$$

where μ is the viscosity of water at the absolute temperature T (Dean, 1992). These new results for O_3 diffusivity are up to 37% larger than previously reported values of Matrozov et al. (1976) who give an average Stokes–Einstein constant of $c = 4.3 \times 10^{-15} Pa \cdot m^2 \cdot K^{-1}$ compared

to $c = 5.9 \times 10^{-15} Pa \cdot m^2 \cdot K^{-1}$ reported here over the temperature range of 20 °C to 30 °C. The discrepancy in c may be explained by the difference in the latest O_3 solubility results used in this analysis. Although these new results obey the Stokes–Einstein equation over small temperature ranges, they are better correlated by an Arrhenius expression over the entire temperature range of this study, as suggested by Reid et al. (1987). The average results for diffusivity are plotted versus temperature on a semilog plot in Figure 2. The error bars correspond to the standard deviations reported in the table. A least-squares regression of the data yielded the following Arrhenius correlation:

$$D/m^2 \cdot s^{-1} = 1.10 \times 10^{-6} \exp[-1896/(TK)] \quad (15)$$

The maximum deviation of the correlation from the mean data is $\pm 3.3\%$.

Literature Cited

- Al-Ghawas, H. A.; Hagewieshe, D. P.; Ruiz-Ibanez, G.; Sandall, O. C. Physicochemical Properties Important for Carbon Dioxide Absorption in Aqueous Methyl-diethanolamine. *J. Chem. Eng. Data* **1989**, *34*, 385–391.
- Bablon, G.; Bellamy, W. D.; Bourbigot, M.; et al. In *Ozone in Water Treatment: Application and Engineering*; Langlais, B., Reckhow, D. A., Brink, D. R., Eds.; Lewis: Chelsea, MI, 1991; Chapter 2.
- Bader, H.; Hoigné, J. Determination of Ozone in Water by the Indigo Method: A Submitted Standard Method. *Ozone Sci. Eng.* **1982**, *4*, 169–176.
- Brink, D. R.; Langlais, B.; Reckhow, D. A. In *Ozone in Water Treatment: Application and Engineering*; Langlais, B., Reckhow, D. A., Brink, D. R., Eds.; Lewis: Chelsea, MI, 1991; Chapter 2.
- Danckwerts, P. V. *Gas-Liquid Reactions*; McGraw-Hill: New York, 1970; pp 32–33.
- Davis, R. A.; Rinker, R. G.; Sandall, O. C. Kinetics of the Reaction of Ozone with 2,4,6-trichlorophenol. *J. Haz. Mat.* **1995**, *41*, 65–72.
- Dean, J. A. *Lange's Handbook of Chemistry*, 14th ed.; McGraw-Hill: New York, 1992; 5.87, p 130.
- Hill, A. G.; Rice, R. G. In *Handbook of Ozone Technology and Applications*; Rice, R. G., Netzer, A., Eds.; Ann Arbor Science: Ann Arbor, MI, 1982; Vol. 1, Chapter 1.
- Incropera, F. P.; DeWitt, D. P. *Fundamentals of Heat and Mass Transfer*, 4th ed.; Wiley: New York, 1996; p 354.
- Kuo, C.; Yocum, F. H. In *Handbook of Ozone Technology and Applications*; Rice, R. G., Netzer, A., Eds.; Ann Arbor Science: Ann Arbor, MI, 1982; Vol. 1, Chapter 5.
- Kuo, C. H.; Li, K. Y.; Wen, C. P.; Weeks, J. L. Absorption and Decomposition of Ozone in Aqueous Solutions. *AIChE Symp. Ser.* **1977**, *166*, 230–241.
- Matrozov, V. I.; Kashtanov, S. A.; Stepanov, A. M.; Tregubov, B. A. Experimental Determination of the Molecular Diffusion Coefficient of Ozone in Water. *J. Appl. Chem. (Leningrad, Russia)* **1976**, *49*, 1070–1073.
- Raimondi, R.; Toor, H. L. Interfacial Resistance in Gas Absorption. *AIChE J.* **1959**, *5*, 86–92.
- Reid, R. C.; Prausnitz, J. M.; Poling, B. E. *The Properties of Gases and Liquids*; McGraw-Hill: New York, 1987; p 615.
- Roth, J. A.; Sullivan, D. E. Solubility of Ozone in Water. *Ind. Eng. Chem. Fundam.* **1981**, *20*, 137–140.

Received for review June 20, 1996. Accepted August 13, 1996.
This work was sponsored by a Grant-in-Aid from the University of Minnesota Graduate School.

JE9602125

© Abstract published in *Advance ACS Abstracts*, September 15, 1996.